

# Correlation Between the Oxygen Content and the Structure of AlCrSiO<sub>x</sub>N<sub>(1-x)</sub> Thin Films Deposited by Pulsed DC Magnetron Sputtering

H. Najafi\*, A. Karimi\* and M. Morstein \*\*

\* Institute of Condensed Matter Physics (ICMP), Ecole Polytechnique Fédérale de Lausanne (EPFL), CH-1015, Lausanne, Switzerland, hossein.najafi@epfl.ch, ayat.karimi@epfl.ch

\*\* Platin AG, Advanced Coating Systems, CH-2545 Selzach, Switzerland, m.morstein@platin.com

## ABSTRACT

Al<sub>52</sub>Cr<sub>40</sub>Si<sub>8</sub>(N<sub>1-x</sub>O<sub>x</sub>) thin films were prepared using pulsed DC magnetron sputtering. Two series of films were deposited at 400°C and 650°C by changing the O/(O+N) in the films from 0% (pure nitrides) to 100% (pure oxides). The obtained films were characterized by various techniques including XRD, XPS, SEM, TEM and nanoindentation. XRD results revealed that in the nitride region, films are crystallized in the cubic (B1) structure, which survives more at 650°C rather than 400°C against the oxygen incorporation. In the transition region between nitrides and oxides, the structure collapses to completely amorphous network and hardness was decreased to 12 GPa. In the oxide region, the formation of nanocrystallites of  $\alpha$ -(Al,Cr)<sub>2</sub>O<sub>3</sub> was observed in particular by the appearance of (113) and (116) reflections in XRD and TEM. The films hardness in this region was increased again to 30-35 GPa.

**Keywords:** oxynitride, XPS, nanoindentation, amorphous network, TEM

## 1 INTRODUCTION

Thin transition metal oxynitride films have led to another class of thin films, which appear to be a simple combination of oxides and nitrides but present new properties and thus allow for outstanding applications [1-3]. Recent years have seen a growing interest in multi element oxynitride films due to their ability to display a variety of properties that cannot be obtained by single-phase films [4]. There are several reasons for choosing multi-element oxynitride films, some of them are diffusion barrier resulting in improved oxidation resistance and chemical stability, thermal barrier, dielectric properties, solid solution hardening and grain size hardening. In this contribution, our aim is to investigate the structural properties of ternary oxynitride thin films of Al-Cr-Si-O-N, covering from pure nitrides to pure oxides. Al-Cr-O-N hard thin films are attracting much attention as the replacement to Ti-Al-O-N films because of the higher solubility of AlN into CrN (i.e. maximum 77%) in the cubic structure (B1) in comparison with the solubility of AlN into TiN (i.e. maximum 65%) system [5]. In our previous research work [6], we studied Al-Cr-Si-O-N system in the hexagonal

crystal structure (B4), whereas currently we are studying this system in the cubic structure. For this purpose, an Al<sub>52</sub>Cr<sub>40</sub>Si<sub>8</sub> target was used to deposit films varying from pure nitrides to pure oxides by changing the O/(O+N) ratio in the films. Then the change in microstructure as well as mechanical properties with the oxygen content are discussed.

## 2 EXPERIMENTAL

The oxynitride thin films were deposited using pulsed DC ( $f = 100$  kHz,  $t = 2 \mu\text{s}$ ) magnetron sputtering of an Al<sub>52</sub>Cr<sub>40</sub>Si<sub>8</sub> target. The [100]-oriented silicon wafer was employed as substrate and a mixed gas of Ar, N<sub>2</sub> and O<sub>2</sub> was applied for sputtering. In order to track the properties of the obtained films from oxygen incorporation, two series of films were deposited at 400°C and 650°C by changing the O<sub>2</sub> / (O<sub>2</sub>+N<sub>2</sub>) ratio in reactive gas from 0% to 100%. The flow rates (sccm) of Ar, N<sub>2</sub> and O<sub>2</sub> gases were controlled via mass flow controller, and the relative partial pressure of reactive gases over the total gas flow was maintained at 30%. Other deposition parameters consisting base pressure in the chamber, working pressure, DC input power and substrate bias were fixed at  $3 \times 10^{-3}$  Pa,  $4.5 \times 10^{-1}$  Pa, 150 W and -50 V, respectively. The films thickness was kept almost the same around 2  $\mu\text{m}$ . The crystallographic structure was investigated by X-ray diffraction using monochromatised CuK $\alpha$  radiation in grazing incidence (4°) geometry. The chemical composition of the achieved films was evaluated via surface X-ray photoelectron spectroscopy (XPS). The XPS data were collected by Axis Ultra (Kratos analytical, Manchester, UK) under ultra-high vacuum condition ( $< 10^{-3}$  Pa), using a monochromatic Al K $\alpha$  X-ray source (1486.6 eV). Gold (Au 4f<sub>7/2</sub>) and copper (Cu 2p<sub>3/2</sub>) lines at 84.0 and 932.6eV, respectively, were used for calibration, and the adventitious carbon 1s peak at 285eV as an internal standard to compensate for any charging effects. Both high resolution scanning electron microscopy (SEM-XLF30-SFEG) operated at 5 kV and transmission electron microscopy (TEM), using Philips CM-20 equipment working at 200 kV, were employed in order to track the microstructures of the selected films. To prepare a suitable sample for TEM, films were thinned by mechanical polishing on diamond pads and then subjected to ion-milling for final thinning up to transparency to the electron

beam. Hardness of samples was determined by the nanoindentor XP with a Berkovitch-type pyramidal diamond tip, indenting the films under continuous stiffness measurement method to a maximum depth of 1000 nm, but the values corresponding to the penetration depth of 100 - 200 nm were assigned as film hardness.

### 3 RESULTS AND DISCUSSION

#### 3.1 Chemical Composition

The atomic composition of the Al-Cr-Si-O-N films was determined from the XPS measurements. Fig. 1a illustrates the chemical composition of films, which were deposited at 650°C versus oxygen fraction ( $O_2/(O_2+N_2)$ ) in the reactive gas. It is noteworthy that there are three different film structures with respect to the oxygen ratio in the reactive gas: nitride films with presence of oxygen in the nitride lattice (cation/anion = 1), films in the transition mode from nitride to oxide structure with no particular lattice, and oxide films with the presence of nitrogen in the oxide lattice (cation/anion = 0.66). The variations of Al/Cr ratio with different oxygen fraction were also plotted in Fig. 1a. It is noticeable that Al/Cr ratios are constant around 1 at lower oxygen fractions (nitride mode), which is lower than the composition of target (i.e. Al/Cr = 1.3). As the oxygen content of the films is raised, the Al/Cr ratio increases from 1 to 1.8 (oxide mode). This could be related to target poisoning that chromium oxide is formed more than aluminum oxide and sputtering of chromium oxide is more difficult than aluminum oxide.

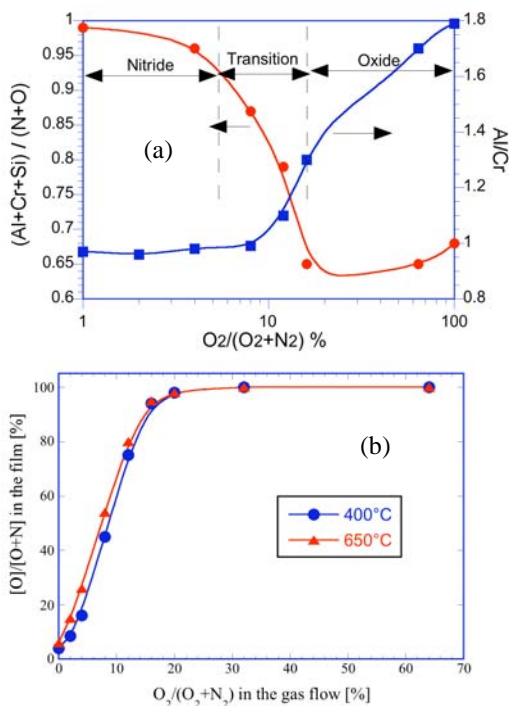


Fig. 1. Variations of cation/anion and Al/Cr ratios of the films (a) and [O]/[O+N] ratio in the films (b) as a function of oxygen fraction ( $O_2 / (O_2+N_2)$ ) in the gas flow.

It is noticeable from Fig. 1b that the incorporation of oxygen into the films increases much faster than the fraction of oxygen in the reactive gas, so that the oxides can be formed from the oxygen fraction of about  $O_2 / (O_2+N_2) = 20\%$ .

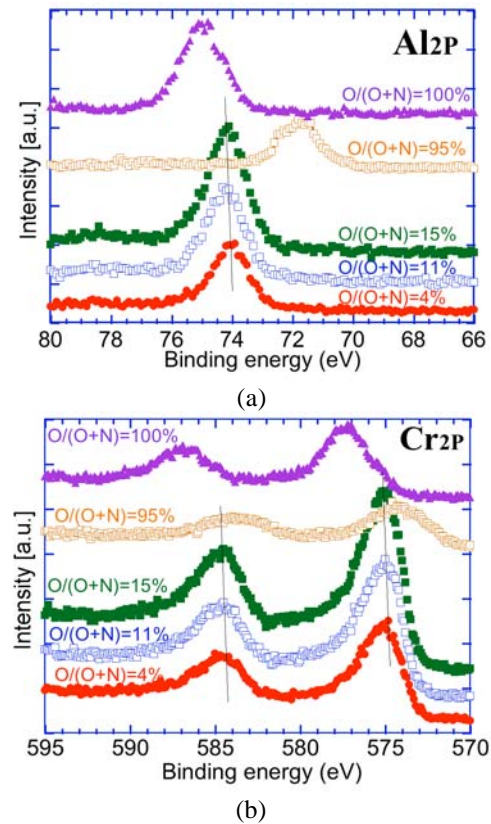


Fig. 2. Al<sub>2p</sub> (a) and Cr<sub>2p</sub> (b) XPS spectra from nitrides to oxides.

Fig. 2a-b shows the chemical environment of the Al and Cr species based on XPS chemical bonding analysis of the Al<sub>2p</sub> and Cr<sub>2p</sub> peaks. The trends of the peak shifts and peak intensities revealed that oxides increase in the film on the expense of nitrides as oxygen was increased. The position and the width of the peaks implied that it contained contributions from both nitride and oxide. Al<sub>2p</sub> and Cr<sub>2p</sub> had a peaks at 74 eV and 575 eV respectively that broadened and shifted to higher energies for increasing oxygen content except for one which corresponds to the transition region that causes the peak to shift to lower energies. This could confirm that chemical environment in the transition region is totally different in comparison to others. In fact at the transition region, quantitative XPS data indicates that stoichiometry of film is much like oxides. As N concentration increases in the expense of oxygen, N may start substituting for O in this bonding configuration. As the valence of N (-3) is substantially more negative than the oxygen valence of -2, this dictates a formal Al valence shifts to a value greater than +3 in the ionic limit of bonding, then the binding energy of electron decreases in XPS measurement [7].

## 3.2 Phase Content and Crystalline Structure

Fig. 3a-b exhibits the grazing incidence XRD spectra of two different series of films deposited at 650°C and 400°C. The results reveal that in both temperatures, nitride films of  $(\text{Al},\text{Cr})\text{N}$  crystallize in the rock salt cubic type of structure (B1) with (111) and (200) peaks being the highest. One can note that the film structure considerably depends on the oxygen fraction. With the increasing of oxygen fraction in the films, the preferred orientation is changed from (111) to (200) as confirmed also by Bragg-Brentano ( $\theta$ - $2\theta$ ) which are not shown here. Furthermore, it is noteworthy that cubic structure survives more at 650°C than 400°C against the oxygen incorporation in the films. This can be described by higher atomic diffusion and crystallinity at high temperatures. In the transition region, films are completely amorphous, as also confirmed by TEM. The oxide films deposited at 650°C exhibit diffused peaks at 43.5° and 57.5° corresponding to (113) and (116) of  $\alpha$ - $(\text{Al},\text{Cr})_2\text{O}_3$ , respectively (pdf n° 43-1484).

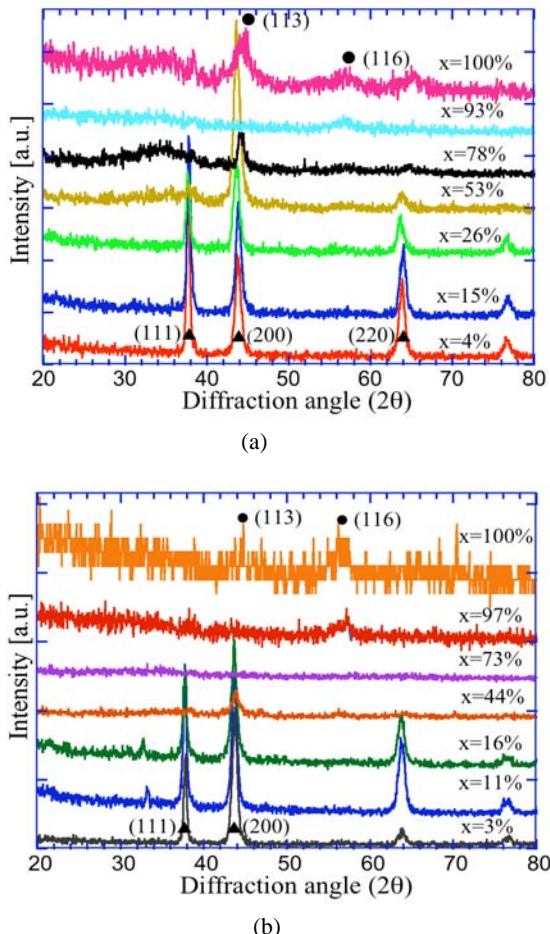


Fig. 3. Grazing incidence XRD patterns of oxynitride films for different concentrations of oxygen  $x=\text{O}/(\text{O}+\text{N})$ , deposited at a) 650°C and b) 400°C. The symbols  $\blacktriangle$  and  $\bullet$  are c-(Al,Cr)N and  $(\text{Al},\text{Cr})_2\text{O}_3$  respectively.

Films deposited at 400°C in oxide region display the existence of  $(\text{Al},\text{Cr})_2\text{O}_3$  in spite of low substrate temperature. These findings are consistent with those reported in [8] confirming the role of Cr in low-temperature growth of  $\text{Al}_2\text{O}_3$ . It is also in accordance with the results of mechanical properties presented in the next sections (Sec. 3.4).

## 3.3 Microscope Study

The morphology of the films deposited at 650°C with different composition has been observed along the plan view SEM and reported in Fig. 4a-c. In the nitride region a granular surface of small crystallites with a grain size of approximately 20 nm was observed. It is noteworthy that at higher oxygen concentrations, for all films initially, the structure collapses into a completely amorphous network followed by the formation of nanocrystallites. This is related to the fact that the mobility of oxygen in the growth surface of amorphous film is not sufficient to form oxide lattice.

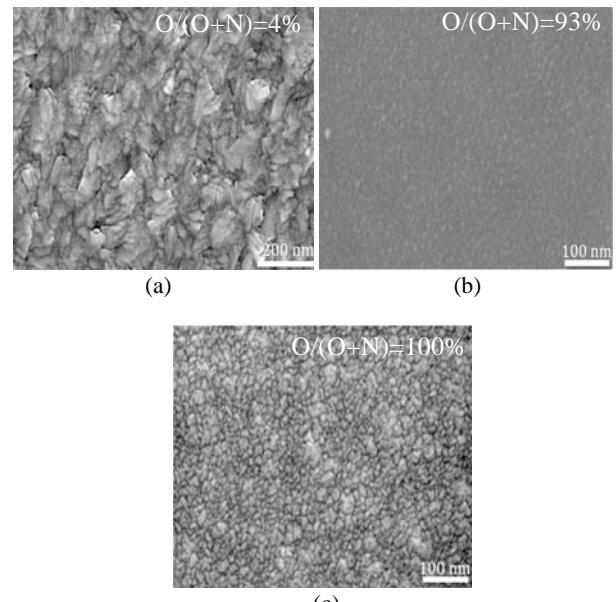


Fig. 4: Plane view SEM micrographs showing microstructure of films with different ratio of  $\text{O}/(\text{O}+\text{N})$  in the film: a)  $\text{O}/(\text{O}+\text{N}) = 4\%$  b)  $\text{O}/(\text{O}+\text{N}) = 93\%$  c)  $\text{O}/(\text{O}+\text{N}) = 100\%$

The TEM cross-sectional image and electron diffraction pattern of the films are shown in Fig. 5. The films containing less oxygen ( $\text{O}/(\text{O}+\text{N}) = 4\%$ ) had a nano-columnar structure (Fig. 5a) and diffraction pattern could be indexed using the cubic (Al,Cr)N rings. According to the Fig. 5b, in the transition region, film was found to be completely amorphous since the diffraction pattern recorded on the film is made of diffuse rings. As depicted in Fig. 5c, films with oxide structure become well-oriented nano-crystalline films and the diffraction pattern could be indexed to (113) and (116) which is in good agreement with the XRD results.

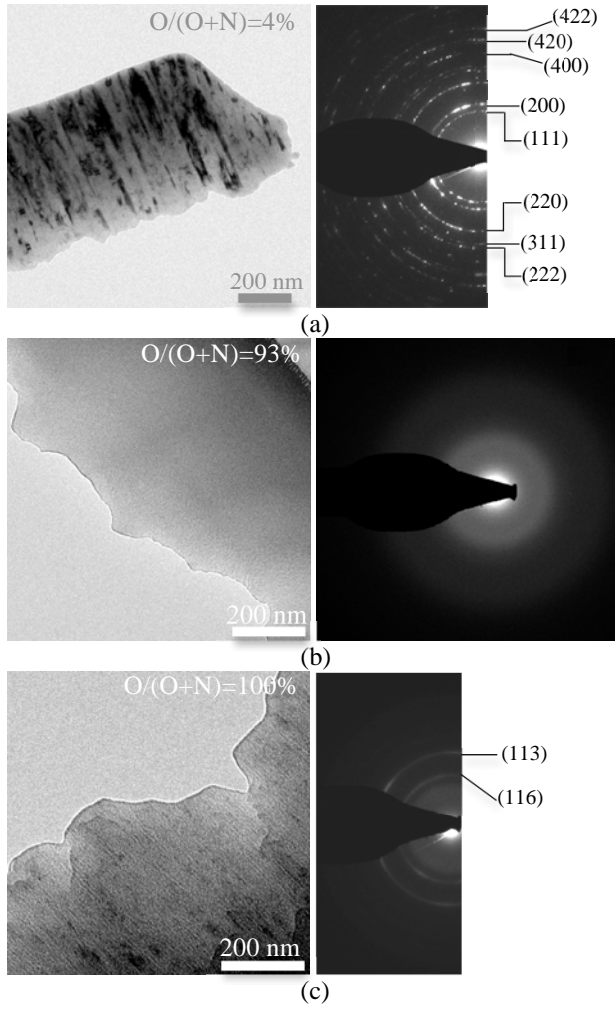


Fig. 5. Cross-sectional TEM micrographs showing the microstructure and diffraction patterns of the films with different ratio of  $O/(O+N)$  in the film: a)  $O/(O+N)=4\%$ , b)  $O/(O+N)=93\%$ , c)  $O/(O+N)=100\%$ ,

### 3.4 Mechanical Properties

The variations of nano-hardness of the films, as a function of oxygen fraction in the reactive gas ( $O_2/(O_2+N_2)$ ) are presented in Fig. 6. The existence of three different modes of films, which correspond to nitride region, transition region and oxide region are obvious as also observed in the chemical analysis and XRD results. For all specimens, as the oxygen fraction increases from 0% to 8%, both hardness and modulus of films alter slightly, this can be dependent to the formation of metal vacancies together with change of chemical bonding in the nitride lattice. Significant decline of hardness from 36 GPa to 16GPa was observed upon increasing the oxygen fraction in the flow gas from 8% to 12%. It is notable that the mechanical properties remain low until the oxygen fraction of 20%. Low mechanical properties of the films in transition mode can be explained by the fact that those are completely amorphous and do not exhibit the peaks of nitride or oxide

phases. By increasing the fraction of oxygen in the reactive gas from 24% to 100% (oxide region), hardness again takes higher values (33-35 GPa), corresponding to the formation of oxides. In the oxide region, films deposited at 400°C exhibit elevated mechanical properties in spite of low temperature for oxide formation. This can be explained by the role of Cr for low-temperature growth of  $(Al,Cr)_2O_3$  [8].

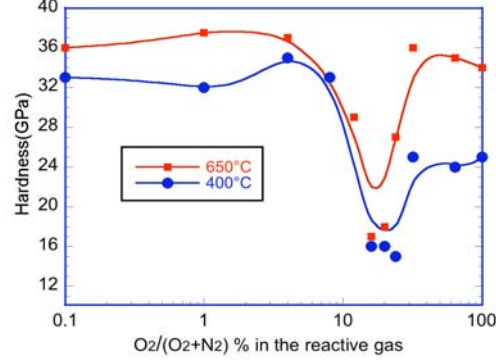


Fig. 6. Hardness of the films as a function of oxygen fraction in the reactive gas for two series of films deposited at 400°C and 650°C.

## 4 CONCLUSION

Both structural and mechanical properties of oxynitride thin films of Al-Cr-Si-O-N were probed versus oxygen concentration. The nitride lattice survives to incorporating of 53% oxygen, and the oxide lattice starts to crystallize when the oxygen content passes beyond 93%. In between, amorphous oxynitride films are formed.

## ACKNOWLEDGEMENTS

The authors are thankful to the Swiss Commission for Technology and Innovation (CTI) for financial support. They would like also to thank CIME-EPFL for providing electron microscopy facilities.

## REFERENCES

- [1] J. Ye, S. Ulrich, C. Ziebert, M. Stüber, Thin Solid Films, 517, 1151, 2008.
- [2] C. C. Lung, C. L. Shu, W. T. Ko, Solid-State Electronics, 50, 103, 2006.
- [3] W. Liu, X. P. Su, S. Zhang, H. B. Wang, J. H. Liu, L. Q. Yan, Vacuum, 82, 1280, 2008.
- [4] A. Karimi, M. Morstein, T. Cselle, Surf. Coat. Technol, In press, 2010.
- [5] Y. Makino, ISIJ Int. 38, 925, 1998.
- [6] H. Najafi, A. Karimi, M. Morstein, Proceeding of 37<sup>th</sup> international conference on metallurgical coatings & thin films, USA, 2010.
- [7] J. R. Smith, P. C. J. Graat, D. A. Bonnell, R. H. French, Mat. Res. Soc. Symp. Proc., 2001.
- [8] J. M. Andersson, E. Wallin, U. Helmersson, U. Kreissig, E. P. Munger, Thin Solid Films, 513, 57, 2006.